Photoluminescence and Charge-Transfer Complexes of Calixarenes Grafted on TiO_2 Nanoparticles

Justin M. Notestein, Enrique Iglesia,* and Alexander Katz*

Department of Chemical Engineering, University of California at Berkeley, Berkeley, California 94720

Received March 21, 2007. Revised Manuscript Received July 3, 2007

Calix[4]arenes and thiacalix[4]arenes, cyclic tetramers of phenol, are synthesized with para position (upper rim) *tert*-butyl, Br, and NO_2 groups and grafted covalently onto surfaces of TiO_2 nanoparticles up to a geometrical maximum surface density of 0.30 nm^{-2}. Grafted calixarenes are hydrolytically stable and are shown to exist in their 'cone' conformation from comparison with model materials synthesized by grafting preformed calixarene−Ti complexes. Individually, protonated calixarenes and TiO_2 absorb only UV light, but calixarene−TiO_2 hybrid organic−inorganic materials absorb light at significantly lower energies in the visible range (>2.2 eV, <560 nm), reflecting ligand-to-metal charge transfer (LMCT) between calixarene and Ti centers on surfaces of TiO_2 nanoparticles. These absorption energies do not depend on the identity and electron-withdrawing properties of upper rim groups in calixarenes. However, the steady-state photoluminescence emission of the calixarene−TiO_2 hybrid material is weakened uniformly throughout the excitation spectrum when compared with the material before calixarene grafting, and these effects become stronger as calixarene upper rim substituents become more electron-withdrawing. The single-step synthesis protocols described here electronically couple calixarenes with surfaces of oxide semiconductors, leading to sensitization of TiO_2 for absorption in the visible region and provide a systematic method for controlling and understanding surface dipole-mediated electron-transfer phenomena relevant to the photocatalytic and optoelectronic properities of TiO_2.

Introduction

The modification of TiO_2 to enhance its ability to absorb photons in the visible spectrum is essential for many applications, including photocatalysis,[1] especially when using solar radiation.[2,3] This can be accomplished by synthesizing TiO_2-based materials with framework substitutions[3,4] or by sensitizing TiO_2 surfaces with an adsorbed dye that transfers electrons from its excited state into the conduction band of the oxide semiconductor.[5] A different type of sensitization occurs when an organic molecule adsorbed on an oxide surface forms a charge transfer (CT) complex that absorbs radiation at a lower energy than either the molecule or the oxide particle. This sensitization occurs by direct injection of an electron from the ground state of the molecule into the conduction band of the particle without involvement of an excited molecular state. Phenols and related compounds are known CT sensitizers for TiO_2,[6−9] and their adsorption geometry and charge-transfer mechanism have been previously explored using spectroscopic, theoretical, and chemical methods.[9−13]

Calixarenes represent a class of macrocyclic phenolic compounds, illustrated in Scheme 1, previously unexplored as TiO_2 sensitizers. Their rich synthetic supramolecular host−guest chemistry[14] and their ability to form complexes with transition metals and main group elements at their lower

* Corresponding author e-mail: askatz@berkeley.edu (A.K.), iglesia@berkeley.edu (E.I.).

(1) Linsebigler, A. L.; Lu, G. Q.; Yates, J. T. *Chem. Rev.* **1995**, *95*, 735−758. Herrmann, J. M. *Top. Catal.* **2005**, *34*, 49−65.
(2) Meyer, G. J. *Inorg. Chem.* **2005**, *44*, 6852−6864.
(3) Anpo, M.; Takeuchi, M. *J. Catal.* **2003**, *216*, 505−516.
(4) Asahi, R.; Morikawa, T.; Ohwaki, T.; Aoki, K.; Taga, Y. *Science* **2001**, *293*, 269−271. Sakthivel, S.; Kisch, H. *Angew. Chem., Int. Ed.* **2003**, *42*, 4908−4911. Belver, C.; Bellod, R.; Stewart, S. J.; Requejo, F. G.; Fernandez-Garcia, M. *Appl. Catal. B* **2006**, *65*, 309−314. Orlov, A.; Tikhov, M. S.; Lambert, R. M. *C. R. Chim.* **2006**, *9*, 794−799. Di Valentin, C.; Pacchioni, G.; Selloni, A. *Chem. Mater.* **2005**, *17*, 6656−6665. Batzill, M.; Morales, E. H.; Diebold, U. *Phys. Rev. Lett.* **2006**, *96*, 26103.
(5) Tributsch, H. *Coord. Chem. Rev.* **2004**, *248*, 1511−1530. Hagfeldt, A.; Gratzel, M. *Acc. Chem. Res.* **2000**, *33*, 269−277.
(6) Kamat, P. V. *J. Phys. Chem.* **1989**, *93*, 859−864. Moser, J.; Punchihewa, S.; Infelta, P. P.; Gratzel, M. *Langmuir* **1991**, *7*, 3012−3018.
(7) Tennakone, K.; Kumara, G. R. R. A.; Kumarasinghe, A. R.; Sirimanne, P. M.; Wijayantha, K. G. U. *J. Photochem. Photobiol. A* **1996**, *94*, 217−220. Tae, E. L.; Lee, S. H.; Lee, J. K.; Yoo, S. S.; Kang, E. J.; Yoon, K. B. *J. Phys. Chem. B* **2005**, *109*, 22513−22522.
(8) Misra, T. K.; Liu, C.-Y. *J. Colloid Interface Sci.* **2007**, *310*, 178−183.
(9) Ikeda, A.; Abe, C.; Torimoto, T.; Ohtani, B. *J. Photochem. Photobiol. A* **2003**, *160*, 61−67.
(10) Kim, S.; Choi, W. *J. Phys. Chem. B* **2005**, *109*, 5143−5149.
(11) Rego, L. G. C.; Batista, V. S. *J. Am. Chem. Soc.* **2003**, *125*, 7989−7997. Liu, Y.; Dadap, J. I.; Zimdars, D.; Eisenthal, K. B. *J. Phys. Chem. B* **1999**, *103*, 2480−2486. Tachikawa, T.; Tojo, S.; Fujitsuka, M.; Majima, T. *Langmuir* **2004**, *20*, 2753−2759. Lana-Villarreal, T.; Rodes, A.; Perez, J. M.; Gomez, R. *J. Am. Chem. Soc.* **2005**, *127*, 12601−12611. Persson, P.; Bergstrom, R.; Lunell, S. *J. Phys. Chem. B* **2000**, *104*, 10348−10351. Rajh, T.; Chen, L. X.; Lukas, K.; Liu, T.; Thurnauer, M. C.; Tiede, D. M. *J. Phys. Chem. B* **2002**, *106*, 10543−10552. Kilsa, K.; Mayo, E. I.; Brunschwig, B. S.; Gray, H. B.; Lewis, N. S.; Winkler, J. R. *J. Phys. Chem. B* **2004**, *108*, 15640−15651. Martin, S. T.; Kesselman, J. M.; Park, D. S.; Lewis, N. S.; Hoffmann, M. R. *Environ. Sci. Technol.* **1996**, *30*, 2535−2542.
(12) Agrios, A. G.; Gray, K. A.; Weitz, E. *Langmuir* **2003**, *19*, 1402−1409.
(13) Rajh, T.; Tiede, D. M.; Thurnauer, M. C. *J. Non-Cryst. Solids* **1996**, *207*, 815−820.
(14) Gutsche, C. D. *Calixarenes*; Royal Society of Chemistry: Cambridge, 1992. Gutsche, C. D. *Calixarenes Revisited*; Royal Society of Chemistry: Cambridge, 1998.

10.1021/cm070779c CCC: $37.00
Published on Web 09/07/2007

Scheme 1. Grafting of Calixarenes onto TiO_2 and SiO_2 Supports[a]

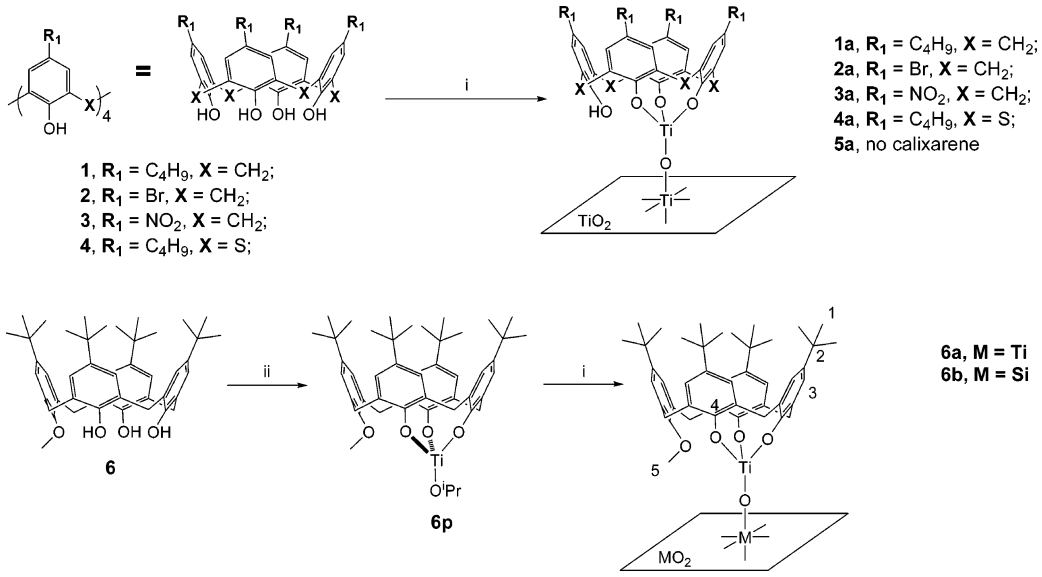

[a] (i) Reflux suspension of TiO_2 and calixarene in toluene under N_2, in the dark, and (ii) add 1 equiv of $TiOPr_4$ at ambient temperature under N_2 for 48 h.

(phenolic) rim[15] make them potential candidates as molecules for semiconductor sensitization. There are many known complexes of *tert*-butylcalixarene derivatives and Ti compounds in which the highly multidentate interaction between a calixarene and Ti leads to very stable complexes.[16] Calixarenes have also been used to measure the concentration of Ti^{4+} ions in aqueous solutions using the ligand-to-metal charge-transfer (LMCT) absorption at ~400 nm arising from complex formation.[17] Some of these calixarene−Ti complexes have been characterized by single-crystal X-ray diffraction,[18,19] which offers structural models for possible adsorption geometries of calixarenes on TiO_2 surfaces. Here, we report the grafting of calixarenes **1**−**4** onto TiO_2 to form stable surface complexes with structures inferred from soluble calixarene−Ti complexes. With these four calixarenes, we tailor the molecular dipole and acidity of the calixarene independently, which allows us to systematically explore the role of surface adsorbed species in modifying electron-transfer processes on (near) the surface of semiconductor particles, such as charge-transfer sensitization and photoluminescence (PL). Understanding these surface phenomena is critical for efficient application of these TiO_2 materials as photocatalysts and optoelectronic materials.

Experimental Methods

Thermogravimetry (TGA) was performed with a TA Instruments TGA 2950 system using a flow of dry synthetic air (0.5 $cm^3\ s^{-1}$ O_2 and 1.5 $cm^3\ s^{-1}$ N_2 as boiloff from liquid) and a Pt pan at a heating rate of 0.083 K s^{-1}. Carbon contents were measured using a Perkin-Elmer 2400 Series II combustion analyzer by the Berkeley Microanalytical Laboratory. Calixarene surface coverages were estimated by determining mass losses between 523 and 1023 K of the oxide material before and after calixarene grafting.

BET surface areas and pore size distributions were determined by N_2 physisorption using a Quantachrome Autosorb 6 after degassing samples overnight at 393 K. UV−visible spectra were measured at ambient conditions and temperature using a Varian Cary 400 Bio UV−visible spectrophotometer with a Harrick Praying Mantis accessory for diffuse reflectance measurements of powders. Compressed poly(tetrafluoroethylene) was used as a perfect reflector standard. PL spectra of dry powders were measured using a Hitachi F-4500 fluorescence spectrophotometer with a front-face solids reflectance accessory at ambient conditions and temperature; a Pyrex filter (UV-32, cutoff at 4.0 eV, 310 nm) was used before the emission detector to remove scattered interference from the excitation beam and its higher harmonics. Emission was measured for excitation wavelengths between 6.2 eV (200 nm) and 2.7 eV (460 nm). Solid-state ^1H MAS and ^{13}C CP/MAS NMR spectra were collected at the California Institute of Technology solid-state NMR facility using a Bruker DSX500 spectrometer at 500 MHz.

Hombikat UV100 (Sachtleben) was chosen as a representative high surface area pure TiO_2 previously used in photocatalysis.[9,10,20]

(15) Wieser, C.; Dieleman, C. B.; Matt, D. *Coord. Chem. Rev.* **1997**, *165*, 93−161; Floriani, C.; Floriani-Moro, R. *Adv. Organomet. Chem.* **2001**, *47*, 167−233.
(16) Takeshita, M.; Shinkai, S. *Bull. Chem. Soc. Jpn.* **1995**, *68*, 1088−1097. Danil de Namor, A. F.; Cleverley, R. M.; Zapata-Ormachea, M. L. *Chem. Rev.* **1998**, *98*, 2495−2525.
(17) Nishida, M.; Yoshida, I.; Sagada, F.; Ishii, D.; Shinkai, S. *Bunseki Kagaku* **1994**, *43*, 295−301.
(18) Dubberley, S. R.; Friedrich, A.; Willman, D. A.; Mountford, P.; Radius, U. *Chem. Eur. J.* **2003**, *9*, 3634−3654. Cotton, F. A.; Dikarev, E. V.; Murillo, C. A.; Petrukhina, M. A. *Inorg. Chim. Acta* **2002**, *332*, 41−46; Radius, U. *Inorg. Chem.* **2001**, *40*, 6637−6642. Clegg, W.; Elsegood, M. R. J.; Teat, S. J.; Redshaw, C.; Gibson, V. C. *J. Chem. Soc., Dalton Trans.* **1998**, *18*, 3037−3039. Zanotti-Gerosa, A.; Solari, E.; Giannini, L.; Floriani, C.; Re, N.; Chiesi-Villa, A.; Rizzoli, C. *Inorg. Chim. Acta* **1998**, *270*, 298−311. Olmstead, M. M.; Sigel, G.; Hope, H.; Xu, X.; Power, P. P. *J. Am. Chem. Soc.* **1985**, *107*, 8087−8091.
(19) Friedrich, A.; Radius, U. *Eur. J. Inorg. Chem.* **2004**, 4300−4316.
(20) Dutta, P. K.; Ray, A. K.; Sharma, V. K.; Millero, F. J. *J. Colloid Interface Sci.* **2004**, *278*, 270−275. Chen, D.; Ray, A. K. *Chem. Eng. Sci.* **2001**, *56*, 1561−1570, Saquib, M.; Muneer, M. *Dyes Pigm.* **2002**, *53*, 237−249. Davydov, L.; Smirniotis, P. G. *J. Catal.* **2000**, *191*, 105−115. Vorontsov, A. V.; Savinov, E. V.; Davydov, L.; Smirniotis, P. G. *Appl. Catal. B* **2001**, *32*, 11−24. Colon, G.; Hidalgo, M. C.; Navio, J. A. *J. Photochem. Photobiol. A* **2001**, *138*, 79−85. Tahiri, H.; Serpone, N.; LevanMao, R. *J. Photochem. Photobiol. A* **1996**, *93*, 199−203. Lindner, M.; Bahnemann, D. W.; Hirthe, B.; Griebler, W. D. *J. Solar Energy Eng. Trans. ASME* **1997**, *119*, 120−125. Lindner, M.; Theurich, J.; Bahnemann, D. W. *Water Sci. Technol.* **1997**, *35*, 79−86. Theurich, J.; Lindner, M.; Bahnemann, D. W. *Langmuir* **1996**, *12*, 6368−6376.

This material is mesoporous (from N_2 physisorption data) with a BET[21] surface area of 340 $m^2\ g^{-1}$. The material is reported by the manufacturer to consist of 12 nm diameter primary crystallites of pure anatase embedded within 50 nm diameter primary particles. The surface titanol density was estimated using TGA to be ~6.5 OH nm^{-2} assuming that mass loss between 393 and 1073 K arises from hydroxyl condensation. The TiO_2 was treated under dynamic vacuum at 393 K for 4 h before use.

Calixarene **1** was purchased from Aldrich (95%). Calixarene **2** was synthesized using methods described elsewhere.[22] Calixarene **3** was synthesized via sulfonation and subsequent nitration[23] of de-*tert*-butylated **1**.[24] Calixarene **4** was synthesized via base-catalyzed condensation of *tert*-butyl phenol with elemental sulfur.[25] Calixarene **6** was synthesized from **1** and iodomethane.[26] All characterization data for these calixarenes matched known literature values.

Calixarene-sensitized TiO_2 materials **1a** and **4a** were synthesized by physically mixing TiO_2 and 0.30 mmol of the corresponding calixarene per g of TiO_2 (0.6 calixarenes per nm^2), suspending the mixture in toluene with magnetic stirring, and refluxing under N_2 for 48 h. For all syntheses, toluene was dried and distilled from CaH_2 before use. The originally white suspension started to turn yellow after ~30 min in reflux, indicative of the presence of CT complexes. The resulting materials **1a** and **4a**, light yellow to orange in color, were washed with boiling toluene and dried under dynamic vacuum for 4 h at ambient temperature. These materials were intentionally synthesized in the presence of excess calixarene to maximize surface densities. The amounts of ungrafted calixarene measured in the wash provided confirmatory estimates for the grafted calixarene surface density measured by TGA. Calixarenes **2** and **3** were poorly soluble in toluene and indeed in most solvents. Therefore, materials **2a** and **3a** were prepared by limiting calixarenes to ~0.12 mmol per g of TiO_2 (~0.2 calixarene per nm^2) during synthesis. These two materials exhibited final calixarene surface densities consistent with quantitative grafting. A portion of material **3a** was additionally washed with copious acetonitrile, methanol/NaOH(aqueous), water, 0.1 N HCl (aqueous), and water to form material **3a-w**. Material **5a** was synthesized using the same procedures but omitting the calixarene, as a control sample.

Material **6a** was synthesized by first adding 1 equiv of $Ti(O^iPr)_4$ (Aldrich 99.999%) to a 0.1 M toluene solution of **6** and stirring under a N_2 atmosphere for 48 h at ambient temperature. This formed the previously described orange-red **6p**.[19] This solution of **6p** was added to TiO_2 (0.25 mmol of **6p** per g of TiO_2), refluxed 24 h in a N_2 atmosphere, and sparged to dryness with N_2 at 388 K. The solids were subsequently washed with excess boiling toluene and dried under dynamic vacuum at ambient temperature for 4 h. Material **6b** was synthesized via the same procedure as **6a** but by replacing TiO_2 with SiO_2 (0.6 nm pore diameter, 250−500 μm particle diameter, partially dehydroxylated under dynamic vacuum at 773 K for 24 h, Selecto Scientific). After contact with calixarene, all TiO_2 materials were handled and stored in foil-wrapped vessels to protect them from light and avoid any photochemical transformations. Materials were stored in sealed screw-top vials but otherwise exposed to ambient air during transfers.

(21) Brunauer, S.; Emmett, P. H.; Teller, E. *J. Am. Chem. Soc.* **1938**, *60*, 309−319.
(22) Gutsche, C. D.; Pagoria, P. F. *J. Org. Chem.* **1985**, *50*, 5795−5802.
(23) Shinkai, S.; Araki, K.; Tsubaki, T.; Arimura, T.; Manabe, O. *J. Chem. Soc., Perkin Trans. 1* **1987**, 2297−2299.
(24) Rathore, R.; Abdelwahed, S. H.; Guzei, I. A. *J. Am. Chem. Soc.* **2004**, *126*, 13582−13583.
(25) Kumagai, H.; Hasegawa, M.; Miyanari, S.; Sugawa, Y.; Sato, Y.; Hori, T.; Ueda, S.; Kamiyama, H.; Miyano, S. *Tetrahedron Lett.* **1997**, *38*, 3971−3972.
(26) Groenen, L. C.; Ruël, B. H. M.; Casnati, A.; Verboom, W.; Pochini, A.; Ungaro, R.; Reinhoudt, D. N. *Tetrahedron* **1991**, *47*, 8379−8384.

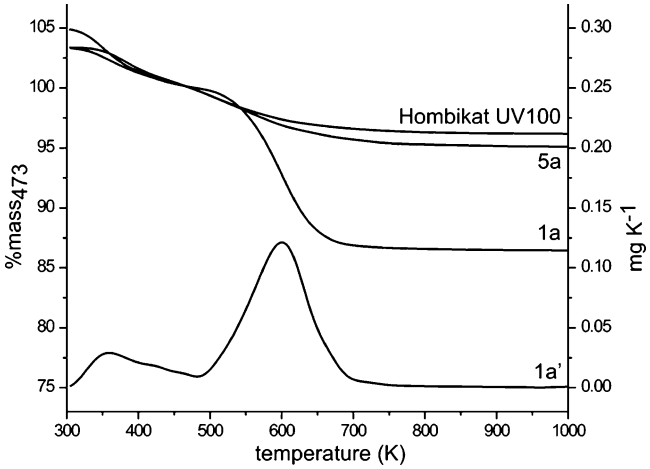

Figure 1. Mass loss of Hombikat UV100, **1a** and **5a** relative to each material's mass at 473 K (top curves), and differential mass loss for **1a** (bottom curve) showing combustion of grafted calixarenes at 500−700 K. There is no significant additional mass loss for material **5a**, which was exposed to synthesis conditions but without calixarene.

Table 1. Physical and Electronic Characterization of Calixarene-Sensitized TiO_2

	calixarene content[a]		edge energy[b] (eV)			
material	mmol g^{-1}	calix nm^{-2}	TiO_2	LMCT	LMCT intensity[c]	PL intensity[d]
Hombikat UV100	0	0	3.33	n/a	0.03	1.0
1a	0.15	0.30	3.24	2.10	0.37	0.73
2a	0.11	0.21	3.20	2.10	0.27	0.52
3a	0.13	0.25	*e*	2.27	3.52	0.36
3a-w	0.04	0.08	3.27	2.13	0.38	
4a	0.13	0.24	3.27	2.20	0.21	0.77
5a	0.02[f]	0.04[f]	3.33	n/a	0.00	1.0
6a	0.11	0.20	3.25	2.20	0.27	0.75
6b	0.14	0.18	n/a	2.22	0.12[g]	n/a[g]

[a] Based on C content and using the surface area of unmodified TiO_2, 343 $m^2\ g^{-1}$. Calculations based on TGA mass loss generally agree to within 10%. [b] ±0.02 eV. [c] At 410 nm (3.0 eV), in KM units. [d] Ratio of the 500 nm (2.5 eV) emission intensity of target material to the 500 nm (2.5 eV) emission intensity of Hombikat UV100 at all excitation energies from 5.8 to 3.5 eV. [e] Obscured by intense LMCT. [f] Expressed as an equivalent amount of calixarene **1**, for comparison purposes. [g] Diluted with 10 g/g SiO_2; PL emission is weak and not strictly comparable to TiO_2-based materials.

Results and Discussion

Figure 1 shows representative TGA data in air for Hombikat UV100 and materials **1a** and **5a**. The surface-grafted calixarenes combust between 500 and 700 K. Calixarene-free **5a** has a similar TGA profile to Hombikat UV100, particularly when compared to the large mass loss for **1a**, indicating that the calixarene molecules, and not residual solvent or other impurities, are responsible for the observed mass loss in materials **1a**−**4a**. Table 1 shows calixarene surface densities represented as mmol g^{-1} of total material and as molecules nm^{-2} of unmodified TiO_2 surface, measured from TGA and BET data and elemental compositions.[27] The calixarene surface densities determined from combustion methods for **1a, 4a**, and **6a** were 0.30, 0.24, and 0.20 nm^{-2}. Extensive washing of **1a** with methanol and water decreased the mass loss upon combustion on TiO_2 samples by <25%; no change was detected after washing in aprotic

organic solvents. This stability is consistent with covalent attachment of calixarenes to TiO_2 surfaces.

N_2 physisorption isotherms at 77 K, pore volume distributions, surface areas, and total pore volumes are reproduced in Figure S2 for selected materials. Material **5a** has surface area and pore volume values within 15% of those for the parent Hombikat UV100, confirming that synthesis protocols did not cause structural changes. In contrast, surface areas were reduced by 1.5 nm^2 and 1.7 nm^2 per calixarene for **1a** and **6a**, respectively, consistent with the cross-sectional area of calixarene **1** estimated from molecular models (1.5 nm^2) and with similar measurements performed previously for calixarenes on SiO_2.[28,29] The slightly higher value for **6a** may reflect the concurrent grafting of calixarenes and isopropoxide groups (detected by ^{13}C CP/MAS NMR spectroscopy) on TiO_2 surfaces. The decrease in TiO_2 pore volume upon grafting (1.35 nm^3 per calixarene) for both materials agrees with the molecular volume for a calixarene (1.3 nm^3). This agreement between the dimensions of calixarene models and the sizes estimated from changes in N_2 absorption is consistent with deposition of isolated calixarenes without pore blocking or reconstruction of TiO_2 particles.

Materials **1a** and **6a** were synthesized in the presence of an excess amount of calixarene. Measured ~0.25 calixarene nm^{-2} surface densities and a calixarene cross-sectional area of ~1.6 nm^2 lead to the conclusion that TiO_2 surfaces are ~40% covered by calixarenes. We have previously demonstrated similar grafting densities and fractional coverages for *tert*-butylcalixarenes on SiO_2.[28−30] This fractional coverage is typical of random irreversible deposition of noninteracting molecules,[31] indicating that the grafting density is limited by the cross-sectional area of a calixarene. These surface coverages are more than 10-fold smaller than the number of TiOH surface groups, indicating that calixarene surface densities are not limited by available surface hydroxyls. Materials **6a** and **6b** were formed from complex **6p**,[19] which is locked into the 'cone' conformation illustrated in Scheme 1. From the similar surface coverages attained for all *tert*-butylcalixarene materials **1a**, **4a**, **6a**, and **6b,** we conclude that all grafted calixarenes are in the same 'cone' conformation that is known to be present for **6a** and **6b**.

Solid-state ^{13}C CP/MAS NMR spectra of **1a** and **6a** are shown in Figure 2. They resemble solution ^{13}C spectra of grafting precursors **1**[32] and **6p**[19] as well as the previously reported spectra for **6b**.[29,33] The solid-state ^{13}C CP/MAS NMR spectrum of **2a**, **3a**, and **4a** (Figure S3) also resemble their respective precursor spectra. Washing these materials with protic solvents causes no significant change in the position or intensity of calixarene resonances. The spectra of **2a** and **3a** show clear evidence for calixarene methylene bridges, confirming that macrocycles were grafted intact. As for calixarenes grafted on SiO_2[28] or resorcinarenes chemisorbed on TiO_2,[8] the broad nature of this resonance indicates structural rigidity, consistent with covalent grafting of intact calixarenes in 'cone' conformations. Resonances A and B at 24 and 71 ppm for **6a** reflect grafted isopropoxide groups from precursor **6p**.[34] Weak resonances at ~161 ppm (labeled 4′) arise from ipso carbons adjacent to phenol oxygens coordinated to Ti[19,29] and provide additional evidence for calixarene−TiO_2 connectivity in **1a**−**4a**, similar to the covalent bonds between calixarenes and Ti atoms in **6a**, **6b**, and precursor molecule **6p**. The solid-state ^1H MAS NMR spectra of all materials (Figure S4) are dominated by a broad signal at ~6 ppm arising from hydrated TiOH surfaces. This signal increased with time of exposure to ambient air after drying; thus, TiO_2 surfaces remain hydrophilic after grafting of hydrophobic calixarenes, as has been previously shown in the case of SiO_2 supports.[28]

The diffuse reflectance UV−visible absorption spectra of the pure TiO_2 precursor and of materials **1a**, **5a**, **6a**, and **6b** are shown in Figure 3. The spectra for other upper rim substituted materials are included in Figure S5. The Kubelka−

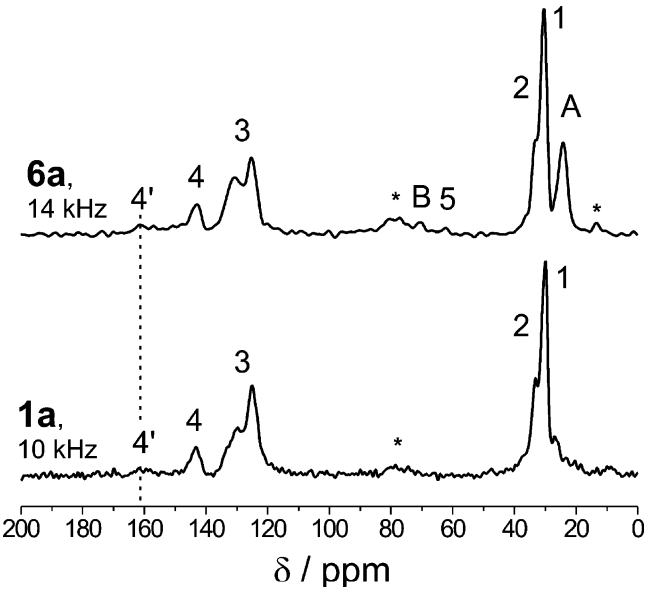

Figure 2. Solid-state ^{13}C CP/MAS NMR spectra of samples **1a** and **6a**. Resonances are labeled to correspond to structure **6a** in Scheme 1. (*) indicates spinning sideband (13 ppm, **6a**) or unidentified species arising from synthesis that is washed off by H_2O/MeOH (78 ppm). Resonances A and B at 24 and 71 ppm indicate the presence of isopropyl groups cografted onto the TiO_2 surface. Resonances corresponding to methylene bridges are obscured by the intense signals from resonances 1 and 2. Other resonances correspond to published solid-state spectra of other grafted calixarene−Ti materials[29,33] and to the published solution spectra of **1**[32] and **6p**.[19] In particular, resonance 4′ indicates a covalent calixarene−Ti complex, which occurs at the same shift (161 ppm, dashed line) for materials synthesized directly (**1a**) and from a precursor approach (**6a**).

(27) For calculating the calixarene content from the TGA, it is assumed that the weight loss between 473 K and 873 K corresponds to loss of a calixarene fragment missing three of the phenolic OH groups. Using this molecular fragment as a basis previously gives a good agreement between carbon contents by combustion analysis and TGA. For TGA and C agreement on material **4a**, it is additionally assumed that the S atoms are ultimately deposited onto the TiO_2 surface and thus do not contribute to the TGA mass loss.

(28) Notestein, J. M.; Katz, A.; Iglesia, E. *Langmuir* **2006**, *22*, 4004−4014.
(29) Notestein, J. M.; Iglesia, E.; Katz, A. *J. Am. Chem. Soc.* **2004**, *126*, 16478−16486.
(30) Katz, A.; Da Costa, P.; Lam, A. C. P.; Notestein, J. M. *Chem. Mater.* **2002**, *14*, 3364−3368.
(31) Fadeev, A. Y.; Lisichkin, G. V. *Stud. Surf. Sci. Catal.* **1996**, *99*, 191−212.
(32) Gutsche, C. D.; Dhawan, B.; No, K. H.; Muthukrishnan, R. *J. Am. Chem. Soc.* **1981**, *103*, 3782−2792.
(33) Notestein, J. M.; Andrini, L. R.; Kalchenko, V. I.; Requejo, F. G.; Katz, A.; Iglesia, E. *J. Am. Chem. Soc.* **2007**, *129*, 1122−1131.
(34) Bouh, A. O.; Rice, G. L.; Scott, S. L. *J. Am. Chem. Soc.* **1999**, *121*, 7201−7210.

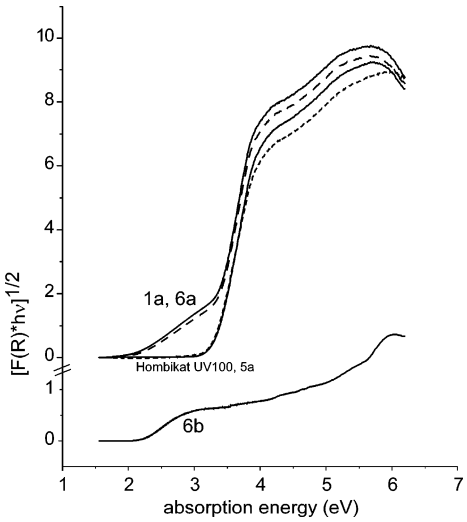

Figure 3. Diffuse reflectance UV−visible absorption of Hombikat UV100 (—), **1a** (—), **5a** (- - -), **6a** (— —), and **6b** (—), assuming materials are indirect semiconductors. F(R) is the pseudoabsorbance calculated using the Kubelka−Munk formalism. Calixarene-containing materials share similar LMCT edge energies of 2.10−2.22 eV. Materials **1a** and **6a** also share similar visible absorption intensities consistent with similar calixarene−Ti surface complexes in both cases. Material **5a** is essentially indistinguishable from Hombikat UV100 indicating no changes to the particle during synthesis in the absence of calixarene.

Munk formalism was used for all powder samples in these figures.[35] The lowest energy transitions corresponding to the band gap of anatase TiO_2 particles are indirect transitions.[36,37] In the calixarene−TiO_2 materials, we use the same formalism to empirically describe the absorption edge energies characteristic of LMCT transitions lower in energy than the band gap. Material **3a** absorbs more intensely in the visible than the other calixarene materials, which prevents an accurate determination of absorption edge for the TiO_2 particle. The energies of the TiO_2 band gap and the LMCT band are therefore measured using the absorption spectrum of alkaline-washed **3a-w** with a lower calixarene surface density (∼0.08 nm^{-2}). The final aqueous HCl wash for this material ensured that no yellow calixarene anions[38] were present and that all color arose from LMCT requiring calixarene−Ti connectivity.

All TiO_2-based materials show an absorption edge at 3.28 ± 0.05 eV (∼375 nm), previously attributed to the indirect transitions in the band gap of anatase TiO_2 nanoparticles.[36] Absorption beyond the inflection point at 4.7 eV (∼265 nm) not only appears to reflect the direct transitions above the band gap in anatase TiO_2[36] but also may arise from defects on the surface or bulk of TiO_2 particles, such as TiOH or undercoordinated Ti^{4+} species also found as isolated Ti atoms within SiO_2 frameworks.[39] Control material **5a** gave no absorption features in the visible region and a band gap identical to that in pure TiO_2 (Hombikat UV100). All synthesis and wash solutions containing residual calixarene gave no absorption features in the visible region (Figure S1). These findings indicate that visible light sensitization in calixarene-containing materials is caused by interactions between calixarenes and surface Ti atoms and not by either of the individual components or by possible artifacts of synthesis conditions, such as the creation of vacancy or substitutional defects in the TiO_2 framework.[3,4]

All calixarene-containing materials give an additional absorption edge in the visible region at 2.15 ± 0.05 eV (∼560 nm), previously attributed to calixarene−Ti LMCT in soluble calixarene−Ti complexes[17] and in material **6b**.[29] This LMCT band is mediated by at least one covalent bond between a calixarene and a surface Ti atom. This band, however, does not distinguish Ti atoms within the TiO_2 framework in **1a** from those grafted onto TiO_2 surfaces in **6a** or onto SiO_2 in **6b**. This band is absent in calixarenes grafted directly onto SiO_2,[28,30] which exhibit no visible absorption, thus confirming that interactions between calixarene and vacant d orbitals on Ti are required for the transitions responsible for these spectral features. For all materials, LMCT energies were insensitive to the identity of the R_1 substituent on the calixarene upper rim (tBu, Br, NO_2). Materials **1a**, **2a**, and **4a** also gave similar LMCT band intensities (Figure S5). Previous studies have shown that substituents on phenols coordinated to d^0 Ti^{4+} atoms do not influence frontier orbitals in Ti centers or their redox potentials,[40] UV−visible spectra, or alkene epoxidation turnover rates, all of which depend on frontier orbital energies at Ti centers.[41]

As in previous studies of catechol adsorption on TiO_2,[42] the known geometries of calixarene−Ti complex **6p**, and of materials **6a** and **6b** derived from it, provide opportunities to probe the details of calixarene−TiO_2 connectivity in directly synthesized material **1a**. In soluble calixarene−Ti complexes such as **6p**, the Ti atom is coordinated simultaneously to three calixarene oxygen atoms each at a distance of ∼0.18 nm (from single-crystal X-ray diffraction[19]), and Ti atoms are four-coordinate in material **6b** (as depicted in Scheme 1 and determined from Ti K-edge X-ray absorption near edge spectroscopy[33]). The similar UV−visible absorption intensities and grafting densities in **1a**, **2a**, **4a**, **6a**, and **6b** require that the absorbing calixarene surface complexes in each of these materials possess similar absorption cross sections. These similarities imply that all materials form multidentate covalent complexes between calixarene and Ti with a geometry as described above, irrespective of whether the complex forms in solution before grafting (**6a** and **6b**) or upon grafting onto TiO_2 surfaces (**1a**). Such a coordination mode for materials **1a**−**4a** requires corner and edge sites on

(35) Delgass, W. N.; Haller, G. L.; Kellerman, R.; Lunsford, J. H. *Spectroscopy in Heterogeneous Catalysis*; Academic Press: New York 1979.
(36) Serpone, N.; Lawless, D.; Khairutdinov, R. *J. Phys. Chem.* **1995**, *99*, 16646−16654. Kumar, P. M.; Badrinarayanan, S.; Sastry, M. *Thin Solid Films* **2000**, *358*, 122−130.
(37) Daude, N.; Gout, C.; Jouanin, C. *Phys. Rev. B* **1977**, *15*, 3229.
(38) Shinkai, S.; Araki, K.; Koreishi, H.; Tsubaki, T.; Manabe, O. *Chem. Lett.* **1986**, 1351−1354.
(39) Anpo, M.; Yamashita, H.; Ichihashi, Y.; Fujii, Y.; Honda, M. *J. Phys. Chem. B* **1997**, *101*, 2632−2636. Marchese, L.; Maschmeyer, T.; Gianotti, E.; Coluccia, S.; Thomas, J. M. *J. Phys. Chem. B* **1997**, *101*, 8836−8838. Corma, A.; Crocker, M.; García, H.; Palomares, E. *ChemPhysChem* **2000**, *2*, 93−97. Soult, A. S.; Carter, D. F.; Schreiber, H. D.; van de Burgt, L. J.; Stiegman, A. E. *J. Phys. Chem. B* **2002**, *106*, 9266−9273.
(40) Fussing, I. M. M.; Pletcher, D.; Whitby, R. J. *J. Organomet. Chem.* **1994**, *470*, 109−117.
(41) Notestein, J. M. Ph.D. Thesis, University of California at Berkeley, 2006.
(42) Wang, Y. H.; Hang, K.; Anderson, N. A.; Lian, T. Q. *J. Phys. Chem. B* **2003**, *107*, 9434−9440.

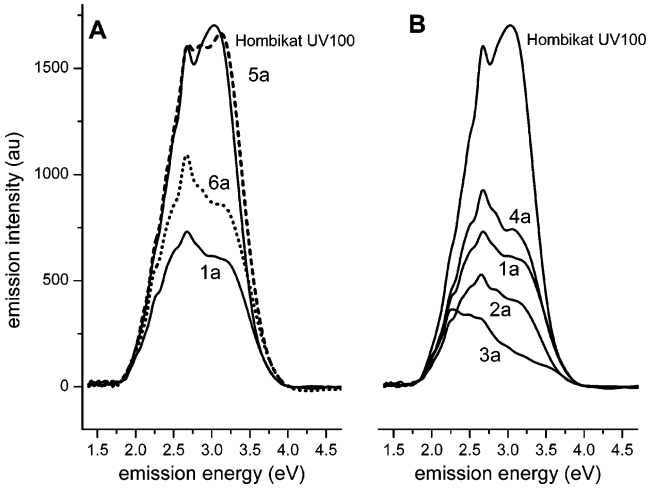

Figure 4. Steady-state PL emission spectra (λ_{ex} = 200 nm, 6.2 eV) of TiO_2-based materials (A) Hombikat UV100, **1a**, and control materials **5a** (— —) and **6a** (- - -) and (B) Hombikat UV100 and **1a**−**4a**. The PL intensity decreases with increasing electron withdrawing ability of the calixarene (**1a**−**3a**), is weakly affected by the mode of attachment to the surface (**1a** vs **6a**), and does not result from handling of the materials (Hombikat UV100 vs **5a**).

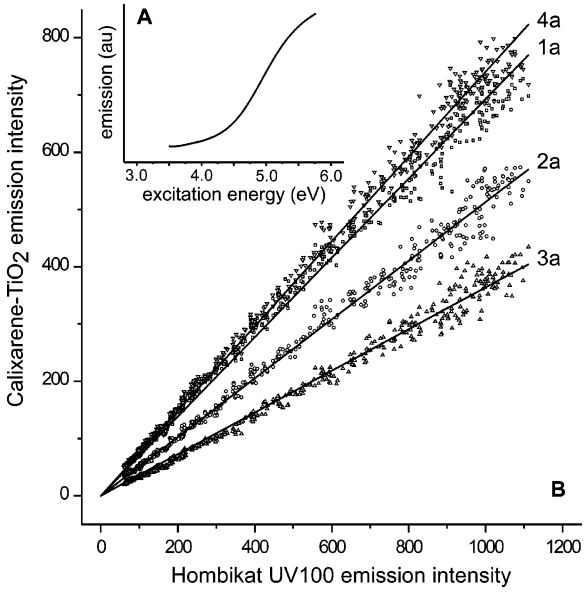

Figure 5. (A) PL excitation spectrum (λ_{em} = 500 nm, 2.5 eV) for Hombikat UV100. (B) Parametric plot of the PL excitation spectra (λ_{em} = 500 nm, 2.5 eV) of materials **1a** (■), **2a** (●), **3a** (▲), and **4a** (▼) versus that of Hombikat UV100 over excitation energies from 5.8 to 3.5 eV illustrating the uniform decrease in PL intensity after calixarene grafting.

small anatase TiO_2 crystallites or regions of amorphous TiO_2, both of which are present in Hombikat UV100 and related materials.[43]

The room-temperature photoluminescence emission spectra of Hombikat UV100 and calixarene-modified materials (Figure 4) show broad emissions between 2.0 and 4.0 eV (600 and 300 nm). Emissions with maxima in the range of 3.0−3.2 eV have been attributed to the band-edge transitions of the anatase crystallite,[44] whereas commonly observed lower-energy emissions (∼2.5 eV) are generally associated with surface or bulk defect sites, including those intrinsic to isolated Ti atoms and titanates;[45] both types of emissions are present simultaneously on certain TiO_2 particles at room temperature and are strongly affected by surface chemistry.[36,46] The spectrum for **5a** (Figure 4A) is identical to that for the untreated Hombikat UV100 TiO_2, consistent with the photoluminescence emission reflecting a species incorporated in the commercial TiO_2 material that is unaffected by dehydration, refluxing, or washing in aprotic nonpolar solvents. Calixarenes grafted onto SiO_2 (without Ti) weakly emit at 310 nm (4.0 eV);[29] no evidence of this emission is seen in materials **1a**−**6a**, consistent with the strong quenching of dye emission by semiconductor oxides.[6,47] The energies of the emission maxima are independent of excitation energy for each material (Figure S6), but the excitation spectra show no clear maximum and increase monotonically for excitation energies above 4.5 eV (Figure 5A, Figure S5). These energies are higher than those of the calixarene−Ti LMCT and the TiO_2 band gap and suggest that the emission arises from the same species and transitions responsible for absorption above 4.7 eV. The emission spectrum (Figure 4A) and excitation spectrum (see Table 1, Figure S5) of **6a** are similar to those of **1a**, indicating that electronic interactions between calixarenes and emitting species on these TiO_2 particles do not distinguish significantly between materials synthesized by direct adsorption or deposition of a preformed complex.

TiO_2 photoluminescence emission intensities strongly decreased upon deposition of the calixarene. Figure 4B shows that the emission became systematically weaker and the overall emission maxima shifted to the red as the calixarene upper rim groups became more electron withdrawing (**4a**∼**1a**>**2a**>**3a**). The emissions at ∼3.0−3.2 eV, attributed to indirect band gap emission and the emissions, at ∼2.6 eV, attributed to surface defects, are both quenched, demonstrating that the calixarene−TiO_2 electronic interaction is not limited merely to surface interactions. Emissions at very low energy (∼2.2 eV) are less strongly affected, suggesting that these emissions arise from isolated bulk defects or impurities in the TiO_2 material. For all examined emission energies, the excitation spectra (Figure 5A) of all materials are strictly proportional to each other, as shown by the parametric plot in Figure 5B. These uniform changes in emission intensity upon calixarene grafting are inconsistent with absorption of excitation or emission energy by calixarene $\pi-\pi^*$ transitions or LMCT, which unlike the observed quenching, depend on incident energy but not on the identity of the calixarene substituent. Because of the similar surface densities and geo-

(43) Chen, L. X.; Rajh, T.; Jager, W.; Nedeljkovic, J.; Thurnauer, M. C. *J. Synchrotron Radiat.* **1999**, *6*, 445−447. Luca, V.; Djajanti, S.; Howe, R. F. *J. Phys. Chem. B* **1998**, *102*, 10650−10657.

(44) Tang, H.; Berger, H.; Schmid, P. E.; Levy, F. *Sol. State Commun.* **1994**, *92*, 267−271. Chandrasekaran, K.; Thomas, J. K. *J. Chem. Soc. Faraday Trans. I* **1984**, *80*, 1163−1172.

(45) Tang, H.; Berger, H.; Schmid, P. E.; Levy, F.; Burri, G. *Solid State Commun.* **1993**, *87*, 847−850. Dehaart, L. G. J.; Devries, A. J.; Blasse, G. *J. Sol. State Chem.* **1985**, *59*, 291−300. Zhang, W. F.; Zhang, M. S.; Yin, Z.; Chen, Q. *App. Phys. B* **2000**, *70*, 261−265. Fujihara, K.; Izumi, S.; Ohno, T.; Matsumura, M. *J. Photochem. Photobiol. A* **2000**, *132*, 99−104. Liu, B. S.; Zhao, X. J.; Wen, L. P. *Mater. Sci. Eng. B* **2006**, *134*, 27−31.

(46) Zhu, Y. C.; Ding, C. X. *J. Solid State Chem.* **1999**, *145*, 711−715. Abazovic, N. D.; Comor, M. I.; Dramicanin, M. D.; Jovanovic, D. J.; Ahrenkiel, S. P.; Nedeljkovic, J. M. *J. Phys. Chem. B* **2006**, *110*, 25366−25370.

(47) Tachibana, Y.; Moser, J. E.; Gratzel, M.; Klug, D. R.; Durrant, J. R. *J. Phys. Chem.* **1996**, *100*, 20056−20062. Hilgendorff, M.; Sundstrom, V. *J. Phys. Chem. B* **1998**, *102*, 10505−10514. Seo, Y. S.; Lee, C.; Lee, K. H.; Yoon, K. B. *Angew. Chem., Int. Ed.* **2005**, *44*, 910−913.

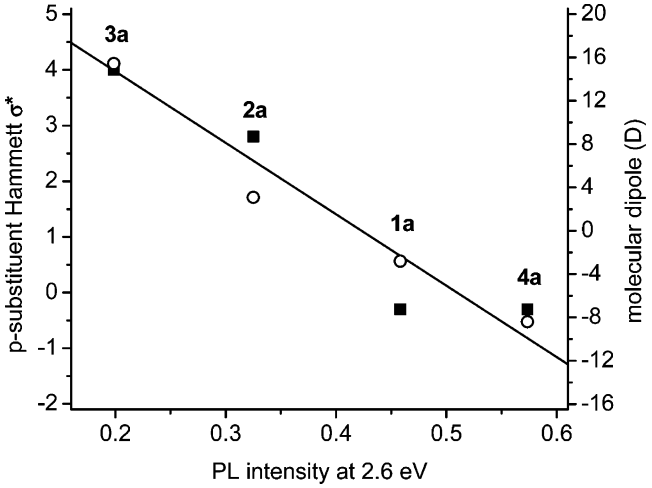

Figure 6. Tabulated values of the Hammett inductive parameter of the upper rim substituent (■) and calculated molecular dipoles of calixarenes **1**−**4** (○) are plotted vs. relative PL emission intensity at 2.6 eV for materials **1a**−**4a** (from Figure 4). Surface dipoles induced by electron withdrawing groups are most consistent with the observed trend.

metric structures of each grafted calixarene, this systematic quenching phenomenon is also inconsistent with incremental changes in the number of emitting species on the surface.

The extent of PL quenching correlates with the Hammett σ^* inductive parameters[48] for the substituent at the calixarene para position and correlates closely with the calixarene molecular dipole (about the 4-fold rotational axis) as calculated by MOPAC using the AM1 Hamiltonian (Figure 6). Changes in the PL of TiO_2 particles have been reported as a function of adsorbed surfactants[49] and of small molecule species involved in aqueous photooxidations.[50,51] PL intensities have been shown to generally decrease with increasing adsorbate electronegativity, but different extents of adsorption and different structures for each adsorbate make systematic correlations difficult. Substituted aromatics adsorbed on metal and semiconductor surfaces have been shown to systematically alter electron-transfer phenomena related to PL, but local effects correlated with adsorbate electronegativity often cannot be distinguished from surface dipolar effects arising from ordered arrangements of the adsorbate molecular dipoles.[42,51,52] Likewise, the observed PL intensity trend **1a** > **2a** > **3a** is consistent with both mechanisms. Similar to an approach taken for understanding modification of indium tin oxide surfaces,[53] we differentiate these two effects by comparing the PL behavior of **1a** and **4a**. The molecular dipole along the calixarene center axis of **4a** is calculated to be more negative than that of any of the calix[4]arenes, consistent with the observed PL intensity (Figure 6). In contrast, thia-calixarene derivatives such as **4** are reported to be more acidic than their calixarene counterparts.[54] Therefore, effects due to the different local atomic composition and higher electronegativity of species on **4a** vs **1a** would be expected to shift **4a** to the left of **1a** in Figure 6 and produce a strong deviation from the given trend line. Thus, the ordering of the PL emission intensities and the nearly identical excitation spectra for **1a** and **4a** are consistent with PL attenuation arising from a systematic increase in the surface dipole as the para substituent of the calixarene becomes more electron withdrawing.

Conclusions

We have demonstrated here that calixarene−Ti complexes are formed on the surface of TiO_2 at up to 0.30 calixarenes nm^{-2} (0.15 mmol calixarenes g^{-1} Hombikat UV100). Because of the 'cone' adsorption geometry and large size of the calixarene, the TiO_2 surface retains residual TiOH groups after calixarene grafting at its maximum density, in contrast with deposition of monomeric phenols,[10,12,55] which in turn suggests preservation of the rich OH radical photochemistry of the TiO_2 surface. The calixarenes are completely resistant to desorption in aprotic solvents or water and quite resistant to washing in alcohols. This stability must be due to the multiple covalent connections possible between Ti surface atoms and a calixarene. Covalent interactions between surface and calixarene are consistent with the appearance of a LMCT absorption in diffuse reflectance UV−visible spectroscopy. The adsorption geometry is deduced from model materials synthesized from preformed calixarene−Ti complexes of known structure. Photoluminescence emission intensities decrease systematically with the increasing electron withdrawing ability of the grafted calixarene, which further demonstrates the involvement of the grafted calixarenes in electronic processes intrinsic to the TiO_2 particle and suggests a surface-dipole governed quenching phenomenon in these systems.

The synthesis method presented here demonstrates a single-step route to covalently and electronically coupling a calixarene host molecule to a TiO_2 nanoparticle. The known oxidative stability of multidentate adsorbates,[13] and the resistance of anchored calixarenes toward desorption should make these materials useful for sensitizing TiO_2 suspensions. Systematic tuning of electron transport properties of the surface is made possible by synthetic calixarenes.[14,56] The host−guest chemistry of cyclodextrins[57] and carciplexes[58] has been used previously to control the interactions between dyes and semiconductor nanoparticles, but the use of calixarenes for controlling the adsorption of molecules onto

(48) Dean, J. A. *Lange's Handbook of Chemistry*, 15th ed.; McGraw-Hill, Inc.: New York, 1999.
(49) Wang, B. Q.; Jing, L. Q.; Qu, Y. C.; Li, S. D.; Jiang, B. J.; Yang, L. B.; Xin, B. F.; Fu, H. G. *Appl. Surf. Sci.* **2006**, *252*, 2817−2825. Wang, Y.; Zhang, S.; Wu, X. H. *Nanotechnology* **2004**, *15*, 1162−1165. Niederberger, M.; Bartl, M. H.; Stucky, G. D. *Chem. Mater.* **2002**, *14*, 4364−4370. Ramakrishna, G.; Ghosh, H. N. *Langmuir* **2003**, *19*, 505−508. Zou, B.; Xiao, L.; Li, T.; Zhao, J.; Lai, Z.; Gu, S. *Appl. Phys. Lett.* **1991**, *59*, 1826−1828.
(50) Shi, J. Y.; Chen, J.; Feng, Z. C.; Chen, T.; Lian, Y. X.; Wang, X. L.; Li, C. *J. Phys. Chem. C* **2007**, *111*, 693−699. Nakajima, H.; Itoh, K.; Murabayashi, M. *Bull. Chem. Soc. Jpn.* **2002**, *75*, 601−606.
(51) Anpo, M.; Tomonari, M.; Fox, M. A. *J. Phys. Chem.* **1989**, *93*, 7300−7302.
(52) Meyer, G. J.; Lisensky, G. C.; Ellis, A. B. *J. Am. Chem. Soc.* **1988**, *110*, 4914−4918. Bruening, M.; Moons, E.; Cahen, D.; Shanzer, A. *J. Phys. Chem.* **1995**, *99*, 8368−8373. Zehner, R. W.; Parsons, B. F.; Hsung, R. P.; Sita, L. R. *Langmuir* **1999**, *15*, 1121−1127. Kruger, J.; Bach, U.; Gratzel, M. *Adv. Mater.* **2000**, *12*, 447.
(53) Bruner, E. L.; Koch, N.; Span, A. R.; Bernasek, S. L.; Kahn, A.; Schwartz, J. *J. Am. Chem. Soc.* **2002**, *124*, 3192−3193.
(54) Matsumiya, H.; Terazono, Y.; Iki, N.; Miyano, S. *J. Chem. Soc., Perkin Trans. 2* **2002**, 1166−1172.
(55) Agrios, A. G.; Gray, K. A.; Weitz, E. *Langmuir* **2004**, *20*, 5911−5917.
(56) *Calixarenes 2001*; Asfari, Z., Ed.; Kluwer: Boston, 2001.

an oxide semiconductor remains unexplored, in spite of a significant precedent for the use of immobilized calixarenes as molecular sensors[59] and binding sites.[60] Given that LMCT interactions are sensitive to the polarity of the local environment,[61] one can envision materials similar to **1a** whose optical absorption, photoaction, or emission spectra are sensitive to guests adsorbed at the calixarene cavity,[28,62] thus creating a novel class of functional nanostructures and sensors.

(57) Lu, P.; Wu, F.; Deng, N. S. *Appl. Catal. B* **2004**, *53*, 87−93. Willner, I.; Eichen, Y.; Frank, A. J. *J. Am. Chem. Soc.* **1989**, *111*, 1884−1886. Willner, I.; Eichen, Y. *J. Am. Chem. Soc.* **1987**, *109*, 6862−6863. Dimitrijevic, N. M.; Rajh, T.; Saponjic, Z. V.; de la Garza, L.; Tiede, D. M. *J. Phys. Chem. B* **2004**, *108*, 9105−9110. Haque, S. A.; Park, J. S.; Srinivasarao, M.; Durrant, J. R. *Adv. Mater.* **2004**, *16*, 1177−1181.

(58) Pagba, C.; Zordan, G.; Galoppini, E.; Piatnitski, E. L.; Hore, S.; Deshayes, K.; Piotrowiak, P. *J. Am. Chem. Soc.* **2004**, *126*, 9888−9889.

(59) *Calixarenes in Action*; Mandolini, L., Ungaro, R., Eds.; Imperial College Press: London, 2000. Grate, J. W.; Patrash, S. J. *Anal. Chem.* **1996**, *68*, 913−917.

(60) *Calixarenes for Separations*; Lumetta, G. J., Rogers, R. D., Gopalan, A. S., Eds.; Oxford University Press: Washington, DC, 2000. Far, A. R.; Cho, Y. L.; Rang, A.; Rudkevich, D. M.; Rebek, J. *Tetrahedron* **2002**, *58*, 741−755. Healy, L. O.; McEnery, M. M.; McCarthy, D. G.; Harris, S. J.; Glennon, J. D. *Anal. Lett.* **1998**, *31*, 1543−1551. Friebe, S.; Gebauer, S.; Krauss, G. J.; Goermar, G.; Krueger, J. *J. Chromatogr. Sci.* **1995**, *33*, 281−284. Ludwig, R. *Fresenius' J. Anal. Chem.* **2000**, *367*, 103−128.

(61) Lever, A. B. P. *Inorganic Electronic Spectroscopy*; Elsevier: New York, 1984.

(62) Shinkai, S. *Pure Appl. Chem.* **1986**, *58*, 1523−1528.

Acknowledgment. We thank Sachtleben for a sample of Hombikat UV100 and Dr. Andrei Solovyov for a sample of **2**. We also acknowledge the financial support of the U.S. DOE Office of Basic Energy Sciences (DE-FG02-05ER15696) and the National Science Foundation (DMR 0444761). We thank Professor Albert Stiegman for helpful technical discussions regarding anatase emission spectra.

Supporting Information Available: UV−visible absorption spectra of homogeneous compounds **1**−**4** and **6p** (Figure S1), N_2 desorption pore volume distributions and adsorption/desorption isotherms for Hombikat UV100 and materials **1a**, **2a**, **5a**, and **6a** (Figure S2), solid-state ^{13}C CP/MAS NMR spectra of materials **2a**, **3a**, and **4a** (Figure S3), solid-state ^{1}H MAS NMR spectra of Hombikat UV100 and materials **1a**−**4a** and **6a** (Figure S4), comparison of diffuse reflectance UV−visible absorption and photoluminescence excitation spectra for Hombikat UV100 and materials **1a**−**4a** (Figure S5), and 3D excitation/emission photoluminescence spectra for Hombikat UV100 and materials **1a**−**4a**. (Figure S6). This material is available free of charge via the Internet at http://pubs.acs.org.

CM070779C